Design of Dual Band Meta-Material Resonator Sensor for Material Characterization

Sucitra R. Harry, Zahriladha Zakaria*, Maizatul Alice M. Said, Rammah Alahnomi, and M. Harris Misran

Microwave Research Group, Centre for Telecommunication Research and Innovation (CeTRI)
Faculty of Electronics and Computer Engineering, Universiti Teknikal Malaysia Melaka (UTeM) Malaysia
*zahriladha@utem.edu.my

Abstract ─ This paper describes the design and implementation of the dual band metamaterial resonator for sensing applications by employing perturbation theory in which the dielectric properties of resonator affect Q-factor and resonance frequency. The designed sensor operates at two resonance frequency 3.20 GHz and 4.18 GHz in the range of 1 GHz to 5.5 GHz for testing solid materials. The Computer Simulation Technology (CST) software is used to design and model this sensor and it was analyzed by using vector network analyzer (VNA) for testing measurement. This study uses empirical equation from the tested materials with well-known permittivity to estimate the permittivity of other materials with unknown permittivity. The proposed sensor has achieved a narrow band with high Q-factor value of 642 and 521 at the operating frequencies of 3.16 GHz and 4.18 GHz respectively. These findings are compared with findings of previous study and the proposed sensor has achieved a high sensitivity and accuracy of 80% compare to others. This is proof that this senor could be used to characterize materials and sensing applications.

Index Terms ─ Dual band, dielectric material characterization, high Q-factor, microwave resonator sensor, solid sample.

I. INTRODUCTION

Microwave sensor for detecting material characterization is the most popular sensor for food industry, quality control, biomedical and industrial application[1]–[3]. Health and safety controls in food products are important to ensure the health and wellbeing of customers which the presence of certain ingredients can affect consumers and cause certain diseases, such as allergies, poisoning and cancer[3]. Due to the reasons above, it is necessary to ensure the quality and safety of the product (e.g., beverages and cooking oils) before marketing them to customers [3]. There are two types of resonant microwave methods for characterizing materials, there are resonant methods and non-resonant methods. Non-resonant method are often used over a frequency range for the electromagnetic properties while resonant method are typically used to correctly understand single frequency or several distinct frequencies of dielectric properties [4].

Microwave resonant technique is one of the potential techniques that is used for highly accurate measurement of dielectric material characterization at single or discrete frequency. The old method states that material characterization has been realized by using conventional waveguide, dielectric and coaxial resonators that have high sensitivity and accuracy [5]. However, the conventional resonator sensor is typically huge, expensive to manufacture and requires a large amount for the detection of the sample of material under test (MUT) [5]–[8]. Thus, planar resonant techniques are among the most common techniques in recent years due to their advantages of compact size, low cost and ease of manufacture [9]–[12]. Moreover, this technique leads to low sensitivity and Q-factor values which restrict the range of material characterization.

The present study was used to find the weaknesses of the previous study through a new microwave sensor that has compatibility, low cost, simple design, easy handling, higher Q-factor, higher accuracy and sensitivity. Therefore, permittivity is a critical function of properties that determine electrical nature of the material. The resonant frequency will be decreasingly shifted to the left from small to large value of permittivity [13], [14].

II. DESIGN METHODOLOGY

A. Structure design

There are two types of designs called design A and design B, which have been successfully investigated and analyzed by the researcher. This microwave resonator sensor is using Roger 5880 with 0.787 thickness, dielectric constant 2.2 and tangent loss 0.0009 as the substrate with dimension 35mm x 25mm which is compact in size. The operating frequency is 3.16 GHz and 4.81 GHz (Design A) and 3.20 GHz and 4.78 GHz (Design B), which is

Submitted On: September 3, 2020
Accepted On: February 14, 2021
https://doi.org/10.47037/2020.ACES.J.360414

from the range 1 GHz to 5.5 GHz.

Before the microwave resonator is designed in the computer simulation technology (CST) software, there are mathematical analysis for the parameter of designation. The frequency of resonance can be determined through the compatible folded arm loading by the length and width of the patch. Thus, length is the parameter that regulates resonant frequency. The length of the of the resonator is half of the wavelength can be expressed in Equation (1) [12]:

$$l = \frac{c}{2\pi\sqrt{\varepsilon_{eff}}} x \frac{1}{f_o}, \quad (1)$$

Whereas the resonant frequency and the effective permittivity that can be calculated in Equation (2) and Equation (3) respectively [15]:

$$f_o = \frac{c}{2\pi r\sqrt{\varepsilon_{eff}}}, \quad (2)$$

$$\varepsilon_{eff} = \frac{\varepsilon_r + 1}{2} + \frac{\varepsilon_r - 1}{2}\left[\frac{1}{1+12\frac{h}{w}}\right]. \quad (3)$$

B. Simulation process

This study used Computer Simulation Technology (CST) to design the sensor. The design of the propose sensor based on the operating frequency, parameter specifications, and the transmission coefficients of the sensor. Parameter value of design sensor as shown in Table 1. When the metamaterial patch size is large, the frequency will be low, then vice versa. Designation on CST design A and design B, as illustrated by Fig. 1 below.

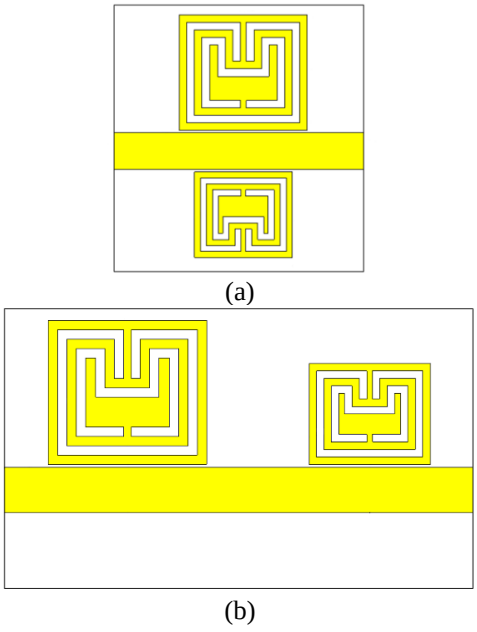

Fig. 1. Designation on CST: (a) design A and (b) design B.

Table 1: Parameter value of design sensor

Substrate	Operating Frequency
Roger 5880	3.16GHz and 4.81GHz (Design A)
	3.20GHz and 4.78GHz (Design B)

Parameter	Design Value	Parameter	Design Value
hs	0.787mm	w	0.5mm
εr	2.2	wk	0.4mm
t	0.0175mm	Cg	0.15mm
Ls	35mm	Dt	17mm
Ws	25mm	g	0.4mm
Lf	35mm	gk	0.3mm
Wf	2.433mm	s	3.4mm
Wr	7.7mm	s2	2.7mm
Lr	8.5mm	la	2.1mm
W2	5.7mm	lb	1.1mm
L2	6.5mm		

In the simulation process, the material under test (MUT) is located at the maximum concentration region of electric field which in red color. Location of MUT at maximum concentration of e-field, as illustrated by Fig. 2 below.

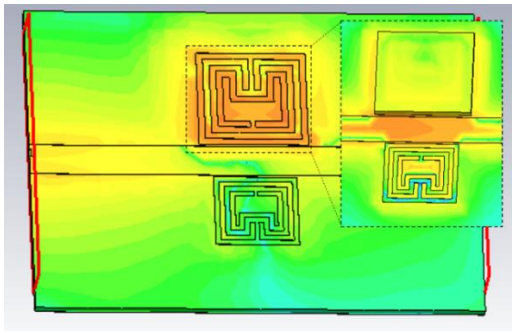

Fig. 2. Location of MUT at maximum concentration of e-field.

C. Measurement process

The microwave resonator sensor is measured by using vector network analyzer (VNA) which analyzed the insertion loss, S21 (dB) of the microwave resonator sensor in the range of frequency 1 GHz to 5.5 GHz. The VNA is connected to the sensor using the two probes station through 50Ω SMA-Connector port of the sensor. The MUT is placed at the top copper of metamaterial patch without touching the feedline in order to avoid other resonant frequency. The dimension for the big MUT is 8.5 mm x 7.7 mm and for the small MUT is 6.5 mm x 5.7 mm. Measurement setup using VNA, as illustrated by Fig. 3 below.

III. RESULTS AND DISCUSSION

A. Q-factor analysis

The resonant frequency shifting determined the accuracy of the microwave resonator sensor. Design A,

resonance frequency for unloaded condition is 3.21 GHz for low frequency and 4.66 GHz for high frequency. However, design B's resonance frequency for unloaded condition is 3.19 GHz for low frequency and 4.69 GHz for high frequency due to coupling loss of gap between feedlines and square patch structure for both designs are 0.15 mm. Therefore, distance between two frequency of design B which is 17 mm also affect resonant frequency shifting of microwave resonator sensor. Low loss occurred when smaller gap between feedline and structure of patch which affect fringing field of perturbation of resonator structure.

Coupling phenomenon between the resonators is also known as mutual coupling which when two patches are coupled through all media such as substrate and air when they are place closed to each other. Comparison result simulation and measurements of design A and design B, as illustrated by Fig. 4 below.

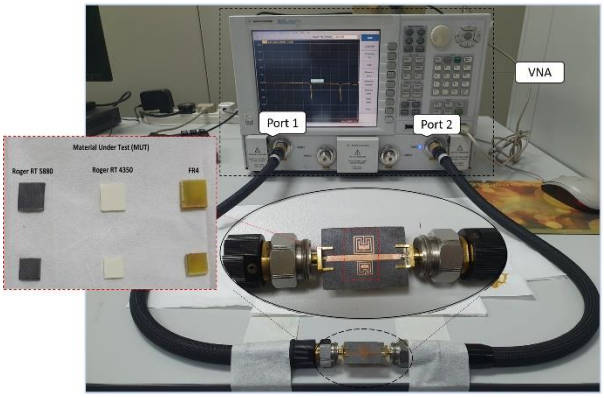

Fig. 3. Measurement setup using VNA.

Design A achieves high quality factor value 350 and 329 for low and high frequency respectively without material under test (MUT). On the other hand, design B achieves high quality factor for low and high frequency are 290 and 278 respectively. Q-factor can be calculated by[16]:

$$Q = \frac{2 f_o}{\Delta f}, \tag{4}$$

where f_o is the resonant frequency and Δf of the resonant peak at -3db. Comparison simulation vs measurement result of low and high frequency (design A & B) as shown in Table 2, Table 3, Table 4 and Table 5.

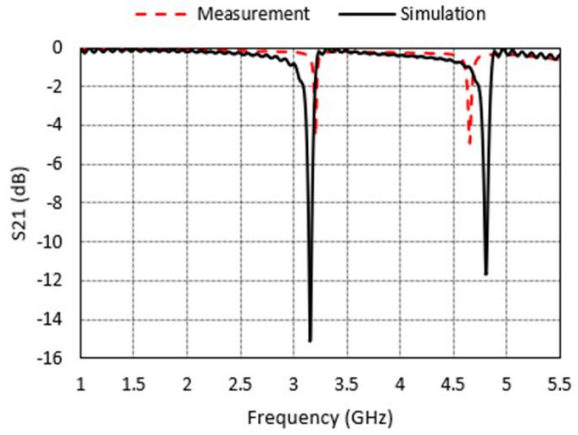

(a)

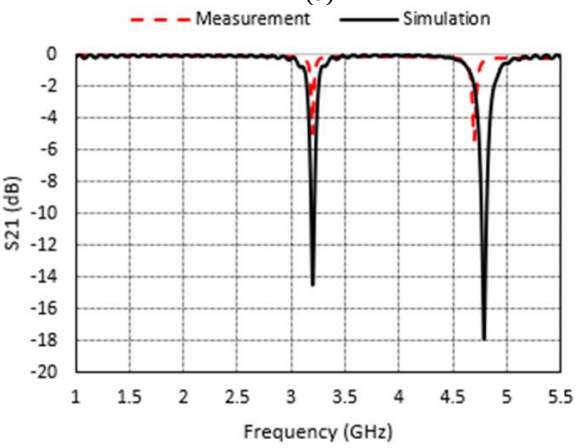

(b)

Fig. 4. Comparison result simulation and measurements of: (a) design A and (b) design B.

Table 2: Comparison simulation vs measurement result of low frequency (design A)

MUT	Simulation						Measurement					
	Q-Factor	S21	BW	f (GHz)	Δf	Error %	Q-Factor	S21	BW	f (GHz)	Δf	Error %
Air	75	-16.959	0.0842	3.16	0	0	350	-4.565	0.0183	3.21	0	0
Roger 5880	70	-16.481	0.0799	2.81	0.35	11.1	642	-3.375	0.0095	3.05	0.16	5
Roger 4350	51	-17.837	0.1009	2.58	0.58	18.3	-	-2.913	-	2.95	0.26	8.1
Fr4	43	-9.227	0.1088	2.34	0.82	26	-	-1.107	-	2.70	0.51	15.9

Table 3: Comparison simulation vs measurement result of high frequency (design A)

MUT	Simulation						Measurement					
	Q-Factor	S21	BW	f (GHz)	Δf	Error %	Q-Factor	S21	BW	f (GHz)	Δf	Error %
Air	113	-13.015	0.0847	4.81	0	0	329	-4.910	0.0283	4.66	0	0
Roger 5880	108	-12.976	0.0786	4.23	0.58	12.1	521	-3.500	0.0168	4.38	0.28	6
Roger 4350	73	-13.771	0.1050	3.83	0.98	20.4	-	-2.832	-	4.35	0.31	6.7
Fr4	64	-6.882	0.1086	3.49	1.32	27.4	-	-0.942	-	3.74	0.92	19.7

Table 4: Comparison simulation vs measurement result of low frequency (design B)

MUT	Simulation						Measurement					
	Q-Factor	S21	BW	f (GHz)	Δf	Error %	Q-Factor	S21	BW	f (GHz)	Δf	Error %
Air	71	-14.496	0.0897	3.20	0	0	290	-5.022	0.0220	3.19	0	0
Roger 5880	107	-13.657	0.0543	2.91	0.29	9.1	474	-3.604	0.0129	3.06	0.13	4.1
Roger 4350	113	-11.503	0.0487	2.74	0.46	14.4	-	-3.003	-	2.92	0.27	8.5
Fr4	121	-4.330	0.0412	2.49	0.71	22.2	-	-1.228	-	2.69	0.5	15.7

Table 5: Comparison simulation vs measurement result of high frequency (design B)

MUT	Simulation						Measurement					
	Q-Factor	S21	BW	f (GHz)	Δf	Error %	Q-Factor	S21	BW	f (GHz)	Δf	Error %
Air	69	-17.911	0.1397	4.78	0	0	278	-5.429	0.0336	4.69	0	0
Roger 5880	102	-14.231	0.0839	4.29	0.49	10.3	380	-4.185	0.0233	4.44	0.25	5.3
Roger 4350	108	-11.302	0.0741	3.99	0.79	16.5	-	-3.346	0.0149	4.40	0.29	6.2
Fr4	137	-4.272	0.0532	3.65	1.13	23.6	-	-1.133	-	3.91	0.78	16.6

B. Analysis dielectric constant and tangent loss analysis

The frequency shift depends on the interference of signal between the maximum concentration of electric fields with the permittivity of the MUT. The measured value of the permittivity value for the MUT have been obtained by using the second order polynomial fitting technique. The difference between reference and the measurement permittivity was analyzed based on percentage error trend line. For design A, the percentage error for permittivity of the samples <12.7% and <26.4% for low frequency and high frequency. For design B, the percentage error for low and high frequency are <5% and <25% respectively.

Loss tangent is the frequency dependent that creates a loss that is proportional to the frequency.

It has higher impact on the peak amplitude S21 when the tangent loss value is smaller. Thus, it makes the S21 parameter narrower when the tangent loss value is smallest. Q-factor of insertion loss is reduced because of the radiation loss that may occur in input and output port network due to the weak connectivity of port couplings and losses occur during fabrication process. Percentage error of losses occur can be calculated in Equation 5:

Comparison permittivity value of reference vs measurement as shown in Table 6. Comparison tangent loss value of reference vs measurement as shown in Table 7. Comparison with previous researcher's sensor as shown in Table 8.

Table 6: Comparison permittivity value of reference vs measurement

MUT	Ref. εr	Measured Permittivity, εr							
		f=3.21 GHz	% Error	f=4.66 GHz	% Error	f=3.19 GHz	% Error	f=4.69 GHz	% Error
Air	1	0.93	7	0.96	4	0.96	4	0.95	5
Roger 5880	2.2	2.48	12.7	2.78	26.4	2.30	4.5	2.75	25
Roger 4350	3.48	3.24	6.9	2.94	15.5	3.40	2.3	2.97	14.7
Fr4	4.4	4.43	0.7	4.41	0.2	4.42	0.5	4.42	0.5

Table 7: Comparison tangent loss value of reference vs measurement

MUT	Ref. Tan δ	Measured Tan δ							
		f=3.21 GHz	% Error	f=4.66 GHz	% Error	f=3.19 GHz	% Error	f=4.69 GHz	% Error
Air	0	0	0	0	0	0	0	0	0
Roger 5880	0.0009	0.000893	0.78	0.000883	1.89	0.000894	0.67	0.000887	1.44
Roger 4350	0.004	0.00399	0.25	0.00398	0.5	0.00398	0.5	0.00399	0.25
Fr4	0.02	0.0199	0.5	0.0199	0.5	0.0199	0.5	0.0199	0.5

Table 8: Comparison with previous researcher's sensor

Ref.	MUT	f (GHz)	Q-Factor	S21 (dB)	E-field	% Accuracy
[16]	Solid	2.50	74	-23.50	Medium	66.2
[17]	Liquid	2.10	130	-13.00	Low	75.8**8**
[18]	Liquid	2.40	-	-35.00	Medium	-
[19]	Solid and Liquid	1.84	49	-2.00	Medium	65.7
[20]	Aqueous Solution	20.00	9.6	-17.77	High	58.5
[21]	Liquid	2.44	146.67	-5.52	Low	78.5
Dual band sensor	Solid	3.16 and 4.18	642 and 521	-3.75 and -3.50	High	>80

IV. CONCLUSION

This paper presented as dual band sensor which proof it can be used to detect the properties of the solid material. Thus, high accuracy and sensitivity sensor works on 3.16GHz and 4.18GHz. This sensor produces a high Q-factor value which are 642 and 541 compared to previous research. A mathematical model is developed for the determination of the dielectric constant and the loss tangent of the MUT. The polynomial curve fitting also applied to determine the dielectric properties of the material. Percentage error for permittivity of measurement

and tangent loss is below 10%. Therefore, percentage of accuracy for this sensor is more than 80% which make the sensor suitable to be apply in further reference.

V. FUTURE WORKS

For further improvement, the sensor can be enhanced by having a portable device to classify the material properties without using the Vector Network Analyzer (VNA) for future suggestions. Thus, it makes the sensor compact in sizes with low cost frequency and can classify the material properties automatically. Then, the sensor also can be enhanced by using algorithms and a Graphical User Interface (GUI) which can read the material characterization of the tested materials. The use of the sensor in the future might be further expanded by measuring the human body's cell tissues, which also involved in dielectric measurement. Thus, this sensor has the high sensitivity which could be used to detect a little change in dielectric properties of the material being tested. The sensor also can be improving by using Internet of Things which allow the user to monitor the material characterization of the tested material.

ACKNOWLEDGMENT

The author gratefully acknowledges the Centre for Research & Innovation Management (CRIM) UTeM, Universiti Teknikal Malaysia Melaka (UTeM) and Ministry of Higher Education (MOHE), Malaysia for funding this work under RACER/2019/FKEKK-CETRI/ F00406.

REFERENCES

[1] S. N. Jha, "Measurement techniques and application of electrical properties for nondestructive quality evaluation of foods-A review," *J. Food Sci. Technol.*, vol. 48, no. 4, pp. 387-411, 2011.

[2] R. A. Alahnomi, Z. Zakaria, E. Ruslan, S. R. A. Rashid, A. Azuan, and M. Bahar, "High - Q sensor based on symmetrical split ring resonator with spurlines for solids material detection," no. c, 2017.

[3] J. Tang, "Unlocking potentials of microwaves for food safety and quality," *J. Food Sci.*, vol. 80, no. 8, pp. E1776-E1793, 2015.

[4] P. M. Narayanan, "Microstrip transmission line method for broadband permittivity measurement of dielectric substrates," *IEEE Trans. Microw. Theory Tech.*, vol. 62, no. 11, pp. 2784-2790, 2014.

[5] U. Schwerthoeffer, R. Weigel, and D. Kissinger, "Microwave sensor for precise permittivity characterization of liquids used for aqueous glucose detection in medical applications," *Microw. Conf.*, vol. 1, no. 4, pp. 1-2, 2014.

[6] K. Shibata and M. Kobayashi, "Measurement of dielectric properties for thick ceramic film on an substrate at microwave frequencies by applying the mode-matchig method," *2016 IEEE MTT-S Int. Conf. Numer. Electromagn. Multiphysics Model. Optim. NEMO 2016*, pp. 1-4, 2016.

[7] A. A. Mohd Bahar, Z. Zakaria, M. K. Md. Arshad, A. A. M. Isa, Y. Dasril, and R. A. Alahnomi, "Real time microwave biochemical sensor based on circular SIW approach for aqueous dielectric detection," *Sci. Rep.*, vol. 9, no. 1, pp. 1-12, 2019.

[8] A. Azuan, M. Bahar, Z. Zakaria, S. Rosmaniza, A. Rashid, and A. A. Isa, "Microstrip planar resonator sensors for accurate dielectric measurement of microfluidic solutions," pp. 416-421, 2016.

[9] M. A. H. Ansari, A. K. Jha, and M. J. Akhtar, "Design and application of the CSRR-based planar sensor for noninvasive measurement of complex permittivity," *IEEE Sens. J.*, vol. 15, no. 12, pp. 7181-7189, 2015.

[10] R. A. Alahnomi, Z. Zakaria, E. Ruslan, and A. A. M. Isa, "Optimization analysis of microwave ring resonator for bio-sensing application," *Int. J. Appl. Eng. Res.*, vol. 10, no. 7, 2015.

[11] R. A. Alahnomi, Z. Zakaria, E. Ruslan, S. R. Ab Rashid, A. A. Mohd Bahar, and A. Shaaban, "Microwave bio-sensor based on symmetrical split ring resonator with spurline filters for therapeutic goods detection," *PLoS One*, vol. 12, no. 9, 2017.

[12] S. Farsinezhad, K. Shankar, M. Daneshmand, and S. Member, "Assisted planar microwave resonator," *IEEE Microw. Wirel. Components Lett.*, vol. 25, no. 9, pp. 621-623, 2015.

[13] A. Iqbal, A. Smida, O. A. Saraereh, Q. H. Alsafasfeh, N. K. Mallat, and B. M. Lee, "Cylindrical dielectric resonator antenna-based sensors for liquid chemical detection," *Sensors (Switzerland)*, vol. 19, no. 5, pp. 2-10, 2019.

[14] J. Yeo and J. I. Lee, "Slot-loaded microstrip patch sensor antenna for high-sensitivity permittivity characterization," *Electron.*, vol. 8, no. 5, 2019, doi: 10.3390/electronics8050502.

[15] K. Chang and L.-H. Hsieh, "Microwave ring circuits and related structures," *Microw. Ring Circuits Relat. Struct.*, 2005, doi: 10.1002/0471721298.

[16] M. A. H. Ansari, A. K. Jha, S. Member, M. J. Akhtar, and S. Member, "Design and application of the CSRR based planar sensor for non-invasive measurement of complex permittivity," no. c, 2015, doi: 10.1109/JSEN.2015.2469683.

[17] W. Withayachumnankul, K. Jaruwongrungsee, A. Tuantranont, C. Fumeaux, and D. Abbott, "Sensors and actuators: A physical metamaterial-based microfluidic sensor for dielectric characterization," *Sensors Actuators A. Phys.*, vol. 189, pp. 233-237, 2013.

[18] M. D. Characterization, A. Ebrahimi, S. Member, and W. Withayachumnankul, "High-sensitivity metamaterial-inspired sensor for," vol. 14, no. 5, pp. 1345-1351, 2014.

[19] G. Galindo-Romera, F. J. Herraiz-Martínez, M. Gil, J. Juan, and D. Segovia-vargas, "Submersible printed split-ring resonator-based sensor for thin-film detection and permittivity characterization," no. c, 2016.

[20] T. Chretiennot, D. Dubuc, and K. Grenier, "A microwave and microfluidic planar resonator for efficient and accurate complex permittivity characterization of aqueous solutions," *IEEE Trans. Microw. Theory Tech.*, vol. 61, no. 2, pp. 972-978, 2013.

[21] A. Kulkarni, "Material characterization using ring resonator," *Int. J. Innov. Res. Comput. Commun. Eng.*, vol. 3, no. 10, pp. 10131-10138, 2015.